

Measurement of $e^+e^- \rightarrow D_s^{(*)+} D_s^{(*)-}$ cross sections near threshold using initial-state radiation

Introduction

- the charmonium states below open charm threshold has been precisely studied and well described by potential models.
- open charm region still not well understood.
- $ee \rightarrow$ charmed-strange meson pair
 - conventional charmonium states
 - parameters were only determined model-dependently by BES
 - Y states have the same spin-parity as charmonium state, but still unexplained well. $ee \rightarrow D_s D_s$ cross sections could play important roles in explaining the inner structure of Y states.

Event Selection

To suppress backgrounds two cases are considered: (1) the γ_{ISR} is outside of the detector acceptance and the polar angle for the $D_s^{(*)+} D_s^{(*)-}$ combination in the c.m. frame is in the range $|\cos(\theta_{D_s^{(*)+} D_s^{(*)-}})| > 0.9$; (2) the γ_{ISR} is within the detector acceptance [$|\cos(\theta_{D_s^{(*)+} D_s^{(*)-}})| < 0.9$]. In the latter case, the γ_{ISR} is required to be detected and the mass of the $D_s^{(*)+} D_s^{(*)-} \gamma_{\text{ISR}}$ combination should be greater than $(E_{\text{c.m.}} - 0.5 \text{ GeV})$. To suppress backgrounds from $e^+ e^- \rightarrow D_s^{(*)+} D_s^{(*)-} (m)(\pi^+ \pi^-) \gamma_{\text{ISR}}$, ($m = 1, 2, \dots$) processes, we exclude events that contain additional charged tracks that were not used in the $D_s^{(*)+}$ and the $D_s^{(*)-}$ reconstruction.

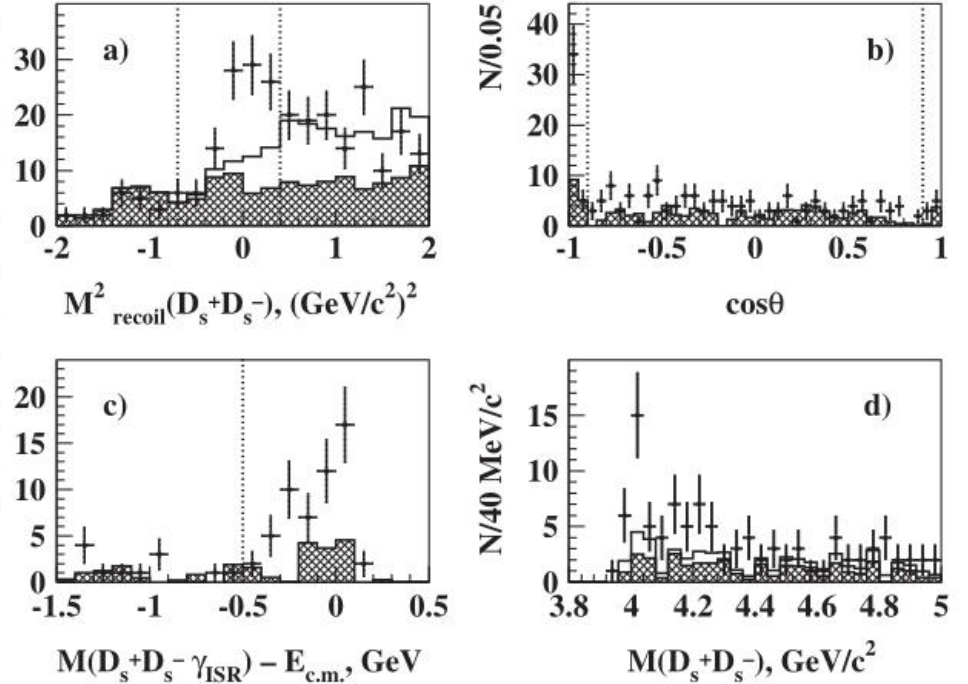


FIG. 1. (a) The distribution of $M_{\text{recoil}}^2(D_s^+ D_s^-)$ for $M_{D_s^+ D_s^-} < 5.0 \text{ GeV}/c^2$ after all the requirements are applied. (b) The polar angle distribution of the $D_s^+ D_s^-$ combinations. (c) The mass spectrum of the $D_s^+ D_s^- \gamma_{\text{ISR}}$ combinations after subtraction of $E_{\text{c.m.}}$ energy in case (2). (d) The $M_{D_s^+ D_s^-}$ spectrum after all the requirements applied. Crosshatched histograms show the normalized $M_{D_s^+}$ and $M_{D_s^-}$ sideband contributions. Feed down from the $D_s^+ D_s^{*-}$ final state is shown by the open histograms. The signal windows are shown by vertical dashed lines.

Event Selection

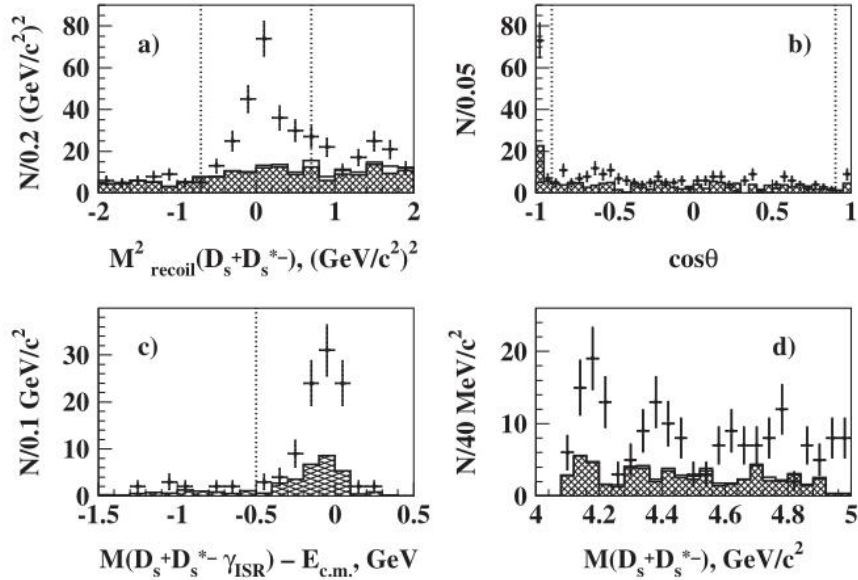


FIG. 2. (a) The distribution of the $M_{\text{recoil}}^2(D_s^+ D_s^{*-})$ for $M_{D_s^+ D_s^{*-}} < 5.0 \text{ GeV}/c^2$ after all the requirements are applied. (b) The polar angle distribution of the $D_s^+ D_s^{*-}$ combinations. (c) The mass spectrum of the $D_s^+ D_s^{*-} \gamma_{\text{ISR}}$ combinations after subtraction of $E_{\text{c.m.}}$ in case (2). (d) The obtained $M_{D_s^+ D_s^{*-}}$ spectrum. Crosshatched histograms show the normalized $M_{D_s^+}$ and $M_{D_s^{*-}}$ sideband contributions. The small contamination from the $D_s^+ D_s^{*-}$ final state is shown by the open histograms. The signal windows are shown by vertical dashed lines.

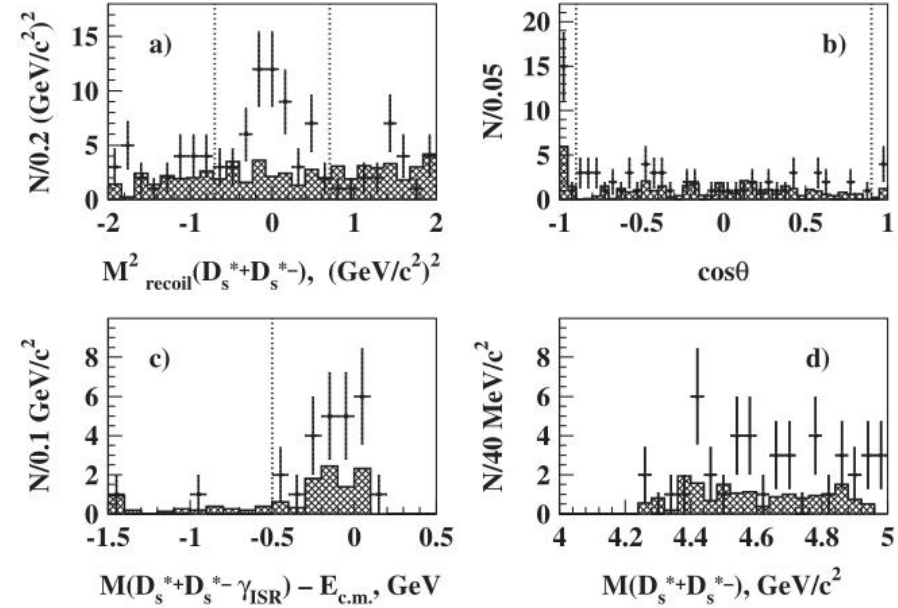


FIG. 3. (a) The distributions of the $M_{\text{recoil}}^2(D_s^{*+} D_s^{*-})$ for $M_{D_s^{*+} D_s^{*-}} < 5.0 \text{ GeV}/c^2$ after all the requirements are applied. (b) The polar angle distribution of the $D_s^{*+} D_s^{*-}$ combinations. (c) The mass spectrum of the $D_s^{*+} D_s^{*-} \gamma_{\text{ISR}}$ combinations after subtraction of $E_{\text{c.m.}}$ in case (2). (d) The $M_{D_s^{*+} D_s^{*-}}$ spectrum after all the requirements are applied. Crosshatched histograms show the normalized $M_{D_s^{*+}}$ and $M_{D_s^{*-}}$ sideband contributions. The signal windows are shown by vertical dashed lines.

cross section

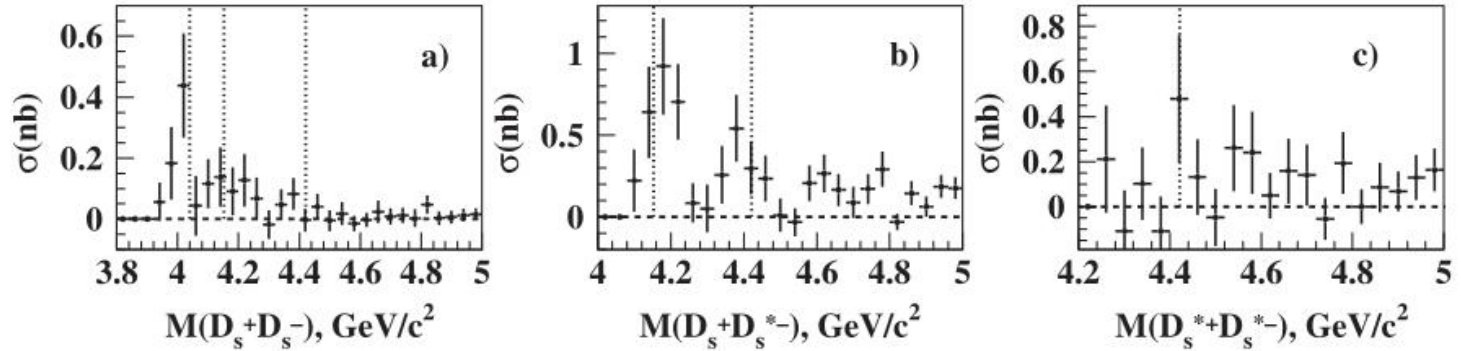


FIG. 4. The cross section averaged over the bin width for (a) the $e^+e^- \rightarrow D_s^+ D_s^-$ process, (b) the $e^+e^- \rightarrow D_s^+ D_s^{*-} + \text{c.c.}$ process, and (c) the $e^+e^- \rightarrow D_s^{*+} D_s^{*-}$ process. Error bars show statistical uncertainties only. There is a common systematic uncertainty for all measurements, 11% for $D_s^+ D_s^-$, 17% for $D_s^+ D_s^{*-}$, and 31% for $D_s^{*+} D_s^{*-}$. This uncertainty is described in the text. The dotted lines show masses of the $\psi(4040)$, $\psi(4160)$, and $\psi(4415)$ states [18].

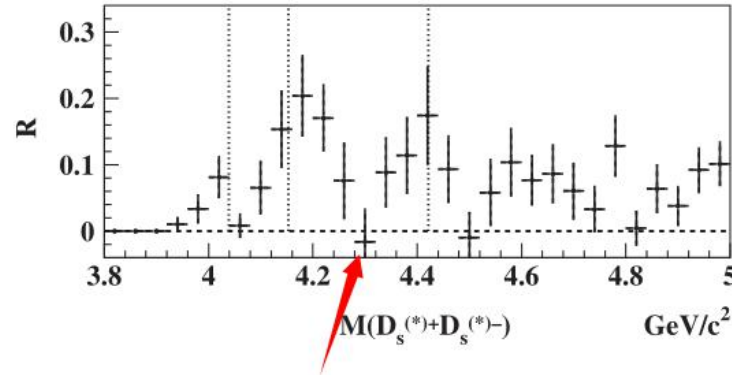
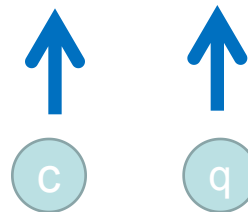
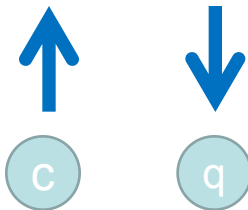


FIG. 5. The R ratio for the sum of the $D_s^+ D_s^-$, $D_s^+ D_s^{*-}$, and $D_s^{*+} D_s^{*-}$ final states. The vertical dotted lines show the masses of the $\psi(4040)$, $\psi(4160)$, and $\psi(4415)$ states [18]. Error bars show statistical uncertainties only.

Question from Yuzhen

- What is the difference of D^{+*} and D^+ ?
- spin of the quarks are different, leading to difference in mass, spin-parity, etc.



Question from Xin

- On page 5, it says “The contribution of final state radiation is strongly suppressed ...”, could you explain why?

The second option to disentangle ISR from FSR exploits the markedly different angular distribution of the photon from the two processes. This observation is completely general and does not rely on any model like sQED for FSR. **FSR is dominated by photons collinear to the final-state particles, while ISR is dominated by photons collinear to the beam direction. This suggests that we should consider only events with photons well separated from the charged final-state particles and preferentially close to the beam** [329, 333, 334].

This is illustrated in Fig. 42, which has been generated running PHOKHARA at leading order (LO). **After introducing suitable angular cuts, the contamination of events with FSR is easily reduced to less than a few per mill.** The price

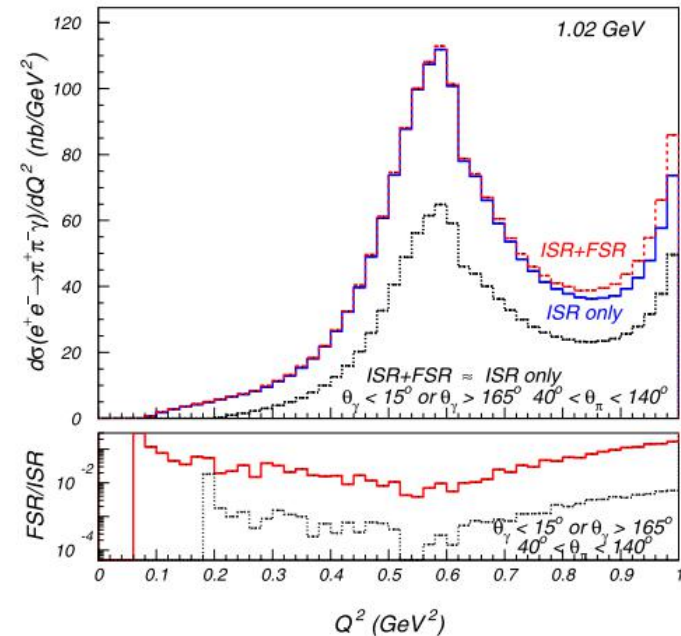


Fig. 42 Suppression of the FSR contributions to the cross section by a suitable choice of angular cuts; results from the PHOKHARA generator; no cuts (*upper curves*) and suitable cuts applied (*lower curves*)

EJTC
The European Physical Journal C
April 2010, Volume 66, Issue 3-4, pp 585-608 | [Cite as](#)

Quest for precision in hadronic cross sections at low energy: Monte Carlo tools vs. experimental data

Authors
Authors and affiliations

Working Group on Radiative Corrections and Monte Carlo Generators for Low Energies, S. Actis, A. Arbuzov, G. Balossini, P. Beltrame, C. Biggiani, R. Bonciani, C. M. Carloni Calame, V. Cherepanov, M. Czakon, H. Czyż, A. Denig, S. Eidelman, G. V. Fedotovich, A. Ferrogli, [show 42 more](#)

Review
First Online: 23 February 2010

484 Downloads
156 Citations

Question from Yuhang

- On page 3, To suppress backgrounds two cases are considered. 1) the γ ISR is outside of the detector acceptance and the polar angle for the $D_s^+ D_s^-$ combination in the c.m. frame is in the range $|\cos(\theta_{D_s^+ D_s^-})| > 0.9$; 2) the γ ISR is within in the detector acceptance $|\cos(\theta_{D_s^+ D_s^-})| < 0.9$. How to understand this.
- momentum conservation.
- the ISR and the $(D_s^+ D_s^-)$ system should be back to back.

Question from Amit

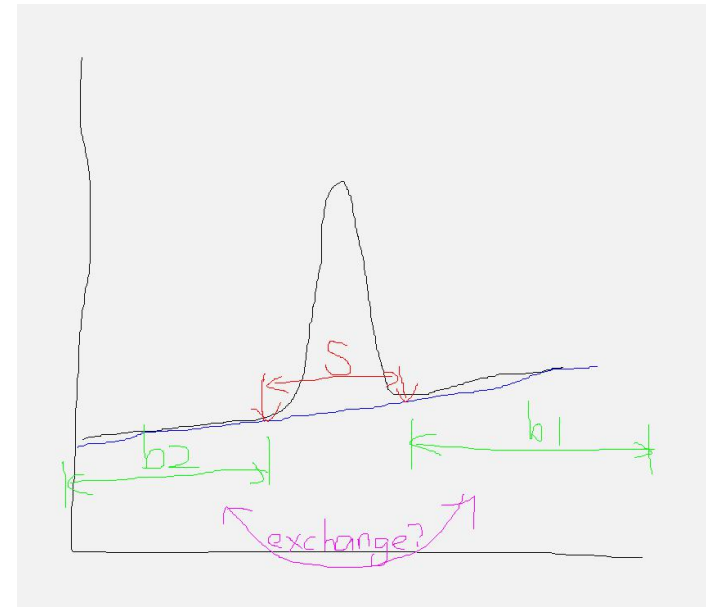
- On Page:- 4
- The following sources of background are considered:
- Point: 3 - The low momentum gamma photon is not reconstructed and
- Point: 4 - The pi0miss is not reconstructed.
- I just want to know, why?
- Is this reconstruction not in the MC simulation or not in the data?

Questions from Suyu

- For the sidebands selection, they used 4 times as large as the signal region, 60MeV, and divided it into windows of the same width as that of the signal, 30MeV. Then they shifted the sidebands, to avoid signal oversubtraction, by 30MeV from the signal region.

From my point of view, 2 sidebands have same parameters of course, e.g. c_0 , c_1 . Does it means that they exchange 2 sidebands(move sideband above the E_{cm} to lower energy side, and another lower than E_{cm} to higher energy side)?

$\eta'\pi^+$. Before calculation of the D_s^+ candidate mass, a vertex fit to a common vertex is performed for tracks that form the D_s^+ candidate. A $\pm 15 \text{ MeV}/c^2$ mass signal window is used for all modes ($\sim 3\sigma$ in each case). To improve the momentum resolution of D_s^+ meson candidates, the tracks from the D_s^+ candidate are fitted to a common vertex with a D_s^+ mass constraint. D_s^{*+} candidates are reconstructed using the $D_s^+\gamma$ decay mode. A $\pm 15 \text{ MeV}/c^2$ mass window is used ($\sim 2.5\sigma$). A mass-constrained fit is also applied to D_s^{*+} candidates.



Question from Shan

- What is the advantage of BESIII compared to Belle in searching for the XYZ states?
- many advantages
 - directly producing Y states
 - larger data sample [main challenge from Belle]
 - precise measurement of state parameters
 - not only simply observe many many new states, but **build the connections between them!**

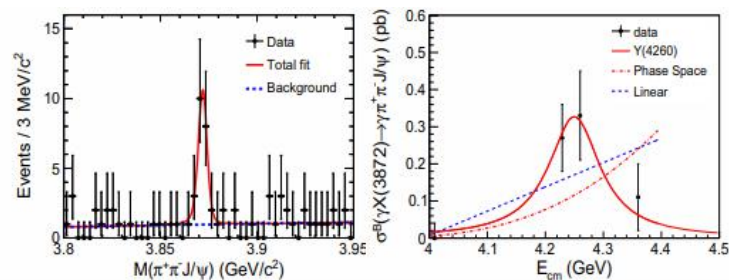


Figure 1: The $\pi^+\pi^-J/\psi$ mass distribution (left). Fit to $\sigma^B[e^+e^- \rightarrow \gamma X(3872)] \times \mathcal{B}[X(3872) \rightarrow \pi^+\pi^-J/\psi]$ with a $Y(4260)$ resonance (red solid curve), a linear continuum (blue dashed curve), or a $E1$ -transition phase space term (red dotted-dashed curve) (right). Dots with error bars are data.

Question from Ryuta

Q. The cross section of $ee \rightarrow D_s D_s$ seems to be one order lower than $ee \rightarrow DD$, however, this paper describes (in the page 1) the one of motivations as "The Y states, ..., provide additional motivation to pursue all possible experimental information about the decomposition of charmed particle production in the charm-threshold region". This description is fine, but thereafter, is there some discussion/paper on Y states (or anything else) where the information of $ee \rightarrow D_s D_s$ result is effectively used ?

Understanding the newly observed $Y(4008)$ by Belle

Xiang Liu*

School of Physics, Peking University, Beijing 100871, China
(Dated: November 11, 2018)

Very recently a new enhancement around 4.05 GeV was observed by Belle experiment. In this short note, we discuss some possible assignments for this enhancement, i.e. $\psi(3S)$ and $D^* \bar{D}^*$ molecular state. In these two assignments, $Y(4008)$ can decay into $J/\psi \pi^0 \pi^0$ with comparable branching ratio with that of $Y(4008) \rightarrow J/\psi \pi^+ \pi^-$. Thus one suggests high energy experimentalists to look for $Y(4008)$ in $J/\psi \pi^0 \pi^0$ channel. Furthermore one proposes further experiments to search missing channels $D\bar{D}, D\bar{D}^* \mp h.c.$ and especially $\chi_{cJ} \pi^+ \pi^- \pi^0$ and $\eta_c \pi^+ \pi^- \pi^0$, which will be helpful to distinguish $\psi(3S)$ and $D^* \bar{D}^*$ molecular state assignments for this new enhancement.

Are $Y(4260)$ and $Z_2^+(4250)$ $D_1 D$ or $D_0 D^*$ Hadronic Molecules?

Gui-Jun Ding

Department of Modern Physics,
University of Science and Technology of China, Hefei, Anhui 230026, China

In this work, we have investigated whether $Y(4260)$ and $Z_2^+(4250)$ could be $D_1 D$ or $D_0 D^*$ molecules in the framework of meson exchange model. The off-diagonal interaction induced by π exchange plays a dominant role. The σ exchange has been taken into account, which leads to diagonal interaction. The contribution of σ exchange is not favorable to the formation of molecular state with $I^G(J^{PC}) = 0^-(1^{--})$, however, it is beneficial to the binding of molecule with $I^G(J^P) = 1^-(1^-)$. Light vector meson exchange leads to diagonal interaction as well. For $Z_2^+(4250)$, the contribution from ρ and ω exchange almost cancels each other. For the currently allowed values of the effective coupling constants and a reasonable cutoff Λ in the range 1-2 GeV, we find that $Y(4260)$ could be accommodated as a $D_1 D$ and $D_0 D^*$ molecule, whereas the interpretation of $Z_2^+(4250)$ as a $D_1 D$ or $D_0 D^*$ molecule is disfavored. The bottom analog of $Y(4260)$ and $Z_2^+(4250)$ may exist, and the most promising channels to discover them are $\pi^+ \pi^- \Upsilon$ and $\pi^+ \chi_{b1}$ respectively.

PHYSICAL REVIEW D 72, 031502(R) (2005)

Four quark interpretation of $Y(4260)$

L. Maiani*

Università di Roma "La Sapienza" and I.N.F.N., Roma, Italy

F. Piccinini†

I.N.F.N. Sezione di Pavia and Dipartimento di Fisica Nucleare e Teorica, via A. Bassi, 6, I-27100, Pavia, Italy

A. D. Polosa‡

Dip. di Fisica, Università di Bari and I.N.F.N., Bari, Italy

V. Riquer§

I.N.F.N., Roma, Italy

(Received 5 July 2005; published 11 August 2005)

We propose that the $Y(4260)$ particle recently announced by BABAR is the first orbital excitation of a diquark-antidiquark state ($[cs][\bar{c}\bar{s}]$). Using parameters recently determined to describe the $X(3872)$ and $X(3940)$ we show that the Y mass is compatible with the orbital excitation picture. A crucial prediction is that $Y(4260)$ should decay predominantly in $D_s \bar{D}_s$. The $Y(4260)$ should also be seen in B nonleptonic decays in association with one kaon. We consider the full nonet of related four-quark states and their predicted properties. Finally, we comment on a possible narrow resonance in the same channel.

DOI: 10.1103/PhysRevD.72.031502

PACS numbers: 12.20.-m, 12.38.-t

$Y(4143)$ is probably a molecular partner of $Y(3930)$

Xiang Liu^{1,2*} and Shi-Lin Zhu^{1†‡}

¹Department of Physics, Peking University, Beijing 100871, China

²Centro de Física Computacional, Departamento de Física,
Universidade de Coimbra, P-3004-516 Coimbra, Portugal

(Dated: November 1, 2018)

After discussing the various possible interpretations of the $Y(4143)$ signal observed by the CDF collaboration in the $J/\psi \phi$ mode, we tend to conclude that $Y(4143)$ is probably a $D_s^* \bar{D}_s^*$ molecular state with $J^{PC} = 0^{++}$ or 2^{++} while $Y(3930)$ is its $D^* \bar{D}^*$ molecular partner as predicted in our previous work [1]. Both the hidden-charm and open charm two-body decays occur through the rescattering of the vector components within the molecular states while the three- and four-body open charm decay modes are forbidden kinematically. Hence their widths are narrow naturally. CDF, Babar and Belle collaborations may have discovered heavy molecular states already. We urge experimentalists to measure their quantum numbers and explore their radiative decay modes in the future.